Chemical Engineering Science, 1959, Vol. 10, pp. 112 to 124. Pergamon Press Ltd. London. Printed in Great Britain

Flow distributions in manifolds

A. Acrivos,* B. D. Babcock† and R. L. Pigford‡

(*Received* 15 *September* 1958)

Abstract—The division of a fluid stream into parts by means of a manifold is accompanied by fluid pressure changes owing to wall friction and to the changing fluid momentum. Friction tends to make the pressure fall while the sudden changes in direction experienced by successive portions of the stream makes the pressure rise in a " blowing " manifold and fall in a " sucking " one. As a result it is not possible to keep the fluid pressure perfectly constant inside the main channel, and there is a consequent variation in the rate of flow through identical ports.

Calculations based on one-dimensional flow equations have been carried out for channels having constant cross-sections, using computing machines. The results are applicable to a wide variety of combinations of channel dimensions, fluid velocity and physical properties, and pressure drop across the side ports. The results are summarized by charts that permit a designer quickly to estimate the non-uniformity in the flow pattern. Predicted distributions agree approximately with observed flow patterns.

Résumé—La division d'un courant fluide au moyen d'une turbulure, est accompagnée d'une variation de pression du fluide due au frottement contre les parois et à la variation de la quantité de mouvement du fluide. Le frottement tend à baisser la pression tandis que les variations brusques de direction vérifée sur des portions successives du courant font augmenter la pression dans le cas d'une tabulure à insuflation, et la fait baisser dans le cas d'une turbulure à aspiration. Il en résulte une impossibilité de rendre la pression du fluide parfaitement constante à l'intérieur du tube, et une variation dans la vitesse d'écoulement à travers les orifices identiques.

Des calculs basés sur des équations découlement à une dimension ont été effectués pour des tuyaux à section constante, à l'aide de machines à calculer. Les résultats sont applicables à un grand nombre de combinaisons de dimensions de tuyaux, vitesse du fluide et propriétés, et chutes de pression par les orifices lateraux. Les résultats sont résumes par des graphiques qui permettent de prévoir rapidement un écoulement non-uniforme. Les distributions prévues ainsi, concordent approximativement avec les écoulements obsérves.

Zusammenfassung—Die Teilung einer strömenden Flüssigkeit durch Verteiler ist von Drückänderungen in der Strömung begleitet, hervorgerufen durch Wandreibung und Impulsänderung. Reibung hat Druckabfall zur Folge, während die plötzliche Richtungsänderung, hervorgerfen durch fortlaufende Strömungsteilung, den Druck in einem " blasenden " Verteiler steigen und in einem " saugenden " Verteiler fallen lässt. Es ist daher nicht möglich, den Flüssigkeitsdruck in der Hauptströmung genau konstant zu halten, was unterschiedliche Strömungsgeschwindigkeiten in gleichgrossen Durchlässen zur Folge hat.

Ausgehend von eindimensionalen Strömungleichusgngen wurden für Kanäle konstanten Durchmessers Rechnungen mit Rechenmaschinen angestellt. Die Ergebnisse sind in einen weiten Bereich verschiedener Kombinationen von Kanalabmessungen, Strömungsgeschwindigkeiten, Stoffeigenschaften und Druckabfall über die seitlichen Durchlässe anwendbar. Die Ergebnisse sind in Diagrammen zusammengefasst, die dem Berechner die schnelle Ermittlung des ungleichförmigen Strömingsverlaufs gestatten. Berechnete Verteilungen stimmen näherungsweise mit dem beobachteten Strömungsverlauf überein.

*Department of Chemistry and Chemical Engineering, University of California, Berkeley, California.
†E.I. du Pont de Nemours and Co., Wilmington, Del.
‡Department of Chemical Engineering, University of Delaware, Newark, Delaware.

Introduction

The design of flow equipment for the division of a fluid stream into several branching streams for the formation of a single, main stream by the confluence of several smaller streams is a problem that is encountered often in chemical processing studies. The simplest device used for these purposes consists of a main, cylindrical channel to which several smaller conduits are attached at right angles. Often the object of the design is to provide for equal flow rates through the several side openings. This can be done if the fluid pressure can be kept constant throughout the main channel; otherwise, each side connection must be provided with a valve to permit adjustments to be made, compensating for the pressure variations within the main channel that would be caused by fluid friction and by the changes in the flow direction and momentum of successive portions of the stream.

As several authors have brought out previously [3, 4, 9] a uniform pressure can be maintained in the main channel by constructing it so that its cross sectional area decreases at a rate that keeps the fluid velocity nearly constant while the mass rate of flow decreases. Although this technique is a useful one it has the disadvantage that a channel designed to give uniform side-ways flow at one flow rate often does not work correctly at another rate. In any case it would appear that computations of the flow distribution to be expected from a manifold constructed from pipe uniform in diameter would be useful to the designer who wishes to provide for *nearly* although not perfectly uniform flow distribution. Frequently it is helpful to know what volume the main channel must have in order that the pressure inside the channel will not vary more than a minimum amount that produces a small but tolerable inequality in flow through the ports.

The differences in fluid pressure arise from two causes: (a) the friction of the fluid against the internal surface of the main channel makes the pressure fall in the direction of flow; and (b) the momentum of the main fluid stream flowing into a manifold tends to carry the fluid toward the closed end, where an excess pressure is produced. When the large fluid stream flows into the manifold and undergoes subdivision (a "blowing manifold") the friction and momentum effects work in opposite directions, the first tending to produce a pressure drop and the second a pressure rise. When the large stream is formed in the manifold by the combination of smaller streams and flows out of the open end of the main channel (a "sucking manifold") the friction and momentum effects reinforce each other, both tending to create lower pressures at the open end than at the closed end. Both friction and momentum effects become more pronounced when the main channel's cross section is reduced while the total quantity of fluid is kept constant. The designer often needs to know how to keep the friction and momentum effects approximately in balance in a blowing manifold and how to estimate the combined effect in a sucking manifold.

This paper describes one-dimensional fluid mechanical calculation methods and pertinent experimental data relating to manifolds of this simplest type, constructed from a main channel of constant cross section that terminates in a closed end and provided with equally spaced, uniformly sized side tubes attached to the main channel at right angles. The manifolds considered either discharge (the "blowing" case) or receive an incompressible fluid (the "sucking" case) from a region in which the pressure is uniform.

Experimental Investigation of the Branching Phenomenon

One of the two principal phenomena affecting the uniformity of fluid pressure inside the manifold is the fluid-momentum effect, which tends to produce a rise in pressure owing to the deceleration of the portion of the fluid that undergoes a change in direction in flowing through a port. The wall shear stress may be nearly the same in the non-porous sections of a manifold as in a long, straight pipe and consequently can be regarded as predictable from existing data on pipe friction. The pressure recovery phenomenon has not been investigated very widely; however, knowledge of the relation between pressure rise and velocity change is essential for the development of the one-dimensional flow theory that follows.

Consider a section of the main channel near

one of the branching outlets as shown in Fig. 1. A momentum balance can be made on the control surface indicated in the figure. If it is assumed that the fluid leaving through the branch has lost

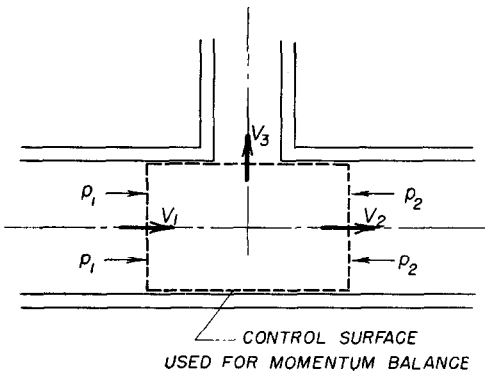

Fig. 1. Fluid pressures and velocities near a manifold port

all its longitudinal component of velocity before it crosses the control surface, the pressure rise, $p_2 - p_1$, is related to the velocity decrease by the equation

$$p_2 - p_1 = \rho\left(\frac{V_1^2 - V_2^2}{g_c}\right) \qquad (0.1)$$

Since the velocity of the side stream may not be exactly in the perpendicular direction when the stream flows through the orifice port it may be expected that the observed pressure rise will be only a fraction, k, of the expected value, so that equation (0.1) should be modified to

$$p_2 - p_1 = k\,\rho\left(\frac{V_1^2 - V_2^2}{g_c}\right) \qquad (0.2)$$

In general k is expected to be smaller than unity.

Although a calculation of the direction of fluid streamlines in the neighborhood of the orifice would permit k to be estimated theoretically, an easier course of action is to determine its value from experimentally observed pressure changes. For this purpose several experiments [1] have been carried out using a 6 ft length of 1·025 in. i.d. brass pipe to which twenty-four side ports were fastened at intervals of 3 in. The side connections were made from 9 in. lengths of 0·317 in. i.d. copper water tubing which were soldered at the top of the main tube over $\frac{1}{4}$ in. diameter holes. Fluid pressures inside the main channel were observed by means of thirty-two pressure taps that were soldered to the bottom of the main tube at 3 in. intervals, taps 5 and 27 being located half-way between side ports 1 and 2 and between 23 and 24, respectively. Connections between the pressure taps and the interior of the manifold were made by drilling $\frac{1}{8}$ in. diameter holes. A sharp-edged orifice was located at a point 28·5 in. upstream from the first side outlet and another was located 31·5 in. downstream from the last outlet. These were used to measure the quantities of air entering and leaving the manifold, respectively, and were calibrated by using a large wet-test meter. The quantity of air leaving any of the side ports could be measured by means of a small-diameter Pitot tube that was also calibrated.

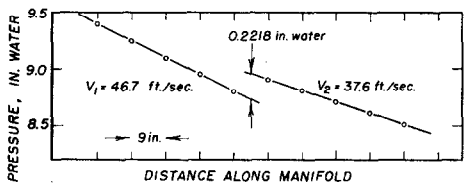

Fig. 2. Typical pressures observed near a single outlet port.

Fig. 2 shows a typical pressure profile observed with only the centre side port, number 13, open. It is seen that the fluid pressure decreases linearly in the direction of flow until the location of the side port is reached. Then a pressure rise occurs, as expected from equation (0.2), and this is followed by a second linear pressure drop. The fall in pressure before and after the port is caused by fluid friction, and the friction factors computed from the pressure gradients were found to be rather closely in agreement with the well established relations for smooth pipe. The effect of the branching flow on the wall friction was not apparent from the data taken and, if present at all, must have been confined to the region within an inch or two of the side port.

Pressure rises caused by the flow branching were calculated from the experimental observations by extrapolating the straight-line pressure profiles to the location of the port and measuring the vertical difference between the lines. When

these values of $p_2 - p_1$ were substituted into equation (0.2) the values of k shown in Fig. 3 were calculated. The fact that the numerical values are less than unity indicates that the streamlines in the diverted stream do not turn a full right angle before the stream leaves the main channel. Some of the force needed to cause the full change in flow direction is apparently produced by excess fluid pressure on the downstream side of the vertical inside surface of the outlet tube.

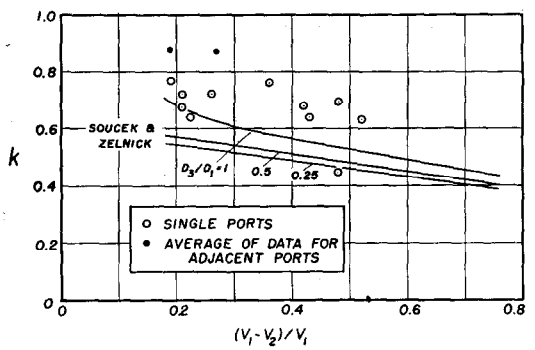

FIG. 3. Pressure recovery coefficients observed in tests of single and double outlet ports.

Fig. 3 also shows lines representing similar data on branching flow as reported by ROUSE [6], based on the work of SOUCEK and ZELNICK [7]. The experiments referred to were made on a long horizontal channel of 6 in. square cross-section through which water flowed. Short side ports were connected to a square channel at right angles. The side ports were square in cross-section and had sharp edges where they were attached to the main channel. In spite of the different geometry and the fluid properties the k-values agree satisfactorily.

A few experiments were made in which two side ports were allowed to discharge simultaneously, leading to data that are shown typically by Fig. 4. The distance between the open ports was varied from 6 in. to 36 in. but there was no significant trend of the k-values for either of the two holes with the spacing between them. The average value for each hole for six different spacings is shown on Fig. 3. The points fall higher than would have been expected from the single-port data. However, the differences between these two points and the previous data are probably not sufficient to affect the predicted flow distribution and an average of all the observations will be used in further calculations.

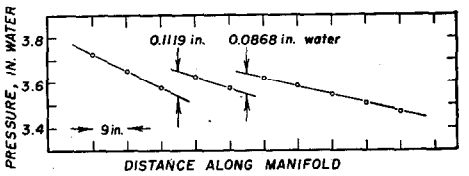

FIG. 4. Typical pressures observed near pair of outlet ports. Fluid velocities before, between and after ports are 28·5, 23·2 and 16·7 ft/sec respectively.

A manifold with a continuously porous wall is a special case of the manifolds under consideration here, in which the number of side tubes is made very large while keeping the ratio of total port area to inside tube surface constant. WEISSBERG [8] has carried out an experimental study of the pressure distribution along the axis of such a manifold through the wall of which air was pumped at a uniform rate. When the pressure loss owing to expected wall friction, using the smooth-tube formula, was subtracted from the observed pressure change, the residual pressure rise was not as large as the net rate of input of fluid momentum. Thus, if equation (0·2) were applied to WEISSBERG's data k-values less than unity would result. In the two experiments where the effect was most noticeable in WEISSBERG's work the appropriate values of k are 0·88 and 0·69, which are of the same order of magnitude as those appearing on Fig. 3.

ONE-DIMENSIONAL FLOW THEORY FOR BRANCHING CONDUITS*

The manifolds of greatest interest here consist of straight tubes with finite numbers of similar side connections spaced equally at discrete

*A more accurately descriptive two-dimensional theory is too difficult to carry out, although laminar-flow calculations can be developed for a case in which the side flow is assumed constant as shown by BERMAN [2]. For rather small side-flow velocities these computations show that the fluid pressure will rise in a "blowing" manifold, in spite of fluid friction, quite like the pressure changes predicted from the simpler, one-dimensional equations.

intervals. When the spacing between the side connections is small, however, and the number of side tubes in any small increment of length is large the manifold can be regarded for all practical purposes as a continuous homogeneous system, equivalent to a main channel having a longitudinal slot or porous strip of constant width. Although the substitution of a continuous for a discrete system may be questionable when the number of side outlets is small the step is justified by the fact that with this simplification the fluid mechanical principles lead to a differential, rather than to a difference equation. Results of computations based on the differential equation can be represented more simply and compactly than is the case for calculations using the non-linear difference equations. However, both types of solutions will be investigated and it will be shown intuitively, as well as mathematically, that the continuous manifolds are but limiting cases of the more interesting, discrete manifolds.

DIFFERENCE EQUATIONS FOR DISCRETE, BLOWING MANIFOLDS

A sketch of a discrete manifold is shown in Fig. 5. The manifold consists of a number of straight-tube sections i, $i+1$, $i+2$, etc., which are separated by an equal number of discharge ports through which fluid leaves the main section of the manifold. The fluid is supposed to flow from left to right and the discharge ports are located at $x = x_i$, where x denotes the distance along the axis of the main tube. Moreover, it will be assumed for simplicity, that the discharge ports are uniformly spaced.

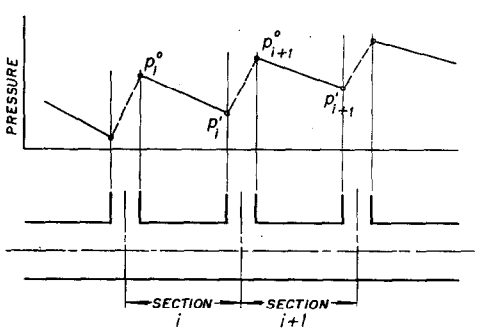

FIG. 5. Nomenclature used for a one-dimensional theory of manifolds.

The Fanning equation is of course applicable to the straight-tube section, so that for section i,

$$p_i' - p_i^\circ = -\frac{2}{g_c}\rho f_i \frac{u_i^2}{D}\Delta x \tag{1.1}$$

On the other hand, a discontinuity in both the pressure and the velocity occurs at $x = x_i$ because of the presence of a discharge port. These changes in the pressure and the velocity can be obtained from a material balance and a momentum balance. Thus if the arithmetic average of pressures just upstream and just downstream from a side port is used to compute the side flow.

$$u_{i+1} - u_i = -\frac{4\alpha C}{D}\Delta x \sqrt{\frac{2g_c}{\rho}\left(\frac{p_i' + p_{i+1}^\circ}{2} - p_0\right)} \tag{1.2}$$

from the orifice equation and a material balance. Also, from a momentum balance, as indicated above,

$$p_{i+1}^\circ - p_i' = \frac{k\rho}{g_c}(u_i^2 - u_{i+1}^2) \tag{1.3}$$

The above three relations are the basic equations for the discrete blowing manifold. They have to be solved, subject to the conditions that at the entrance of the manifold

$$u = u_0$$

and

$$p = p_0' \tag{1.4}$$

These equations can, however, be considerably simplified if a change is made in both the independent and the dependent variables. Thus, letting

$$y \equiv \left(\frac{4\alpha C}{D}\sqrt{2k}\right)x \tag{1.5}$$

$$P_i^\circ \equiv \frac{g_c}{2k\rho u_0^2}(p_i^\circ - p_0) \tag{1.6}$$

$$U_i \equiv \frac{u_i}{u_0} \tag{1.7}$$

the basic equations become

$$P_i' - P_i^\circ = -F_i U_i^2 \Delta y \tag{1.8}$$

where $$F_i \equiv \frac{f_i}{2^{5/2}k^{3/2}\alpha C} \tag{1.8a}$$

$$U_{i+1} - U_i = -\Delta y\sqrt{P_i' + P_{i+1}^\circ} \tag{1.9}$$

and

$$P^{\circ}_{i+1} - P'_i = \tfrac{1}{2}(U_i^2 - U_{i+1}^2) \qquad (1.10)$$

Next, by combining equation (1.9) and (1.10) one finds that

$$U_{i+1} = \frac{1}{1 + \frac{(\Delta y)^2}{2}} \times \left\{ U_i - \sqrt{\frac{(\Delta y)^4}{4} U_i^2 + 2(\Delta y)^2 \cdot \left[1 + \frac{(\Delta y)^2}{2}\right] P'_i} \right\} \qquad (1.11)$$

while, at the entrance of the manifold.

$$U_0 = 1$$

and $$P^{\circ}_1 = \frac{M_0^2}{2} = \frac{g_c(p'_0 - p_0)}{2k\,\rho u_0^2} \qquad (1.12)$$

Finally,* equations (1.8), (1.10) and (1.11), subject to the conditions given by equation (1.12), can be solved by a stepwise numerical iteration. This can vary easily be programmed for a digital computer like the Bendix G-15-D machine for example. The closed end of the manifold is at the point where $U = 0$.

It is seen, then, that the change of variables effected by equations (1.5), (1.6) and (1.7) enables one to formulate the problem mathematically in terms of only three dimensionless parameters, namely M_0, F_0 and Δy, where M_0 is related to the pressure and fluid momentum at the open end of the manifold, F_0 is related to the friction in the straight-tube section, and Δy is related to the distance between adjacent discharge ports. Numerical results for this problem, in terms of the above three parameters, are given below.

Differential Equations for Continuous, Blowing Manifolds

So far, the discussion has been confined to discrete manifolds only. However, the special, continuous case merits attention, because of its relative simplicity. These manifolds, as was mentioned above contain a very large number of discharge ports along the main tube. The mathematical equations for this special case can readily be obtained from the basic equations for the discrete manifold by letting $\Delta x \to 0$ while keeping α, the fractional discharge area, constant.

Thus, as $\Delta y \to 0$, equations (1.8), (1.10) and (1.13) can be combined formally* to give

$$\frac{dP}{dy} + U\frac{dU}{dy} + F_0 U^{7/4} = 0 \qquad (1.14)$$

while, equation (1.9) becomes formally

$$\frac{dU}{dy} = -\sqrt{2P} \qquad (1.15)$$

These last two relations can finally be combined to give the basic differential equation for the continuous, blowing manifold.

$$\left(\frac{d^2U}{dy^2}\right)\left(\frac{dU}{dy}\right) + U\left(\frac{dU}{dy}\right) + F_0 U^{7/4} = 0 \qquad (1.16)$$

with the conditions that, at $y = 0$

$$U = 1 \qquad (1.17)$$

and $$\frac{dU}{dy} = -M_0$$

Equation (1.16) is now a non-linear, second-order, ordinary differential equation which, can easily be integrated numerically. Again, a digital computer, like the Bendix, can readily be employed with advantage in carrying out the numerical computations. The solution to this problem is expressible in terms of only two dimensionless parameters, namely M_0 and F_0, Δy having been eliminated in the limiting process. Therefore, as one would have expected intuitively the basic equation for the continuous manifold can be obtained as a limiting form from equations (1.8), (1.9) and (1.10), by formally letting $\Delta y \to 0$. Equation (1.16) can, however, also be derived directly, that is independently of the relations for the discrete manifold, by making a momentum balance on a differential element of volume in the main channel.

*If we assume that the friction factor varies with fluid velocity according to the generally accepted relationship for smooth tubes we should write

$$F_i = F_0 U_i^{-1/4}. \qquad (1.13)$$

*The purely formal limiting process outlined below can be justified rigorously, although the details will be omitted here.

Sucking Manifolds

In this section the basic equations for both the discrete and the continuous sucking manifolds will be briefly derived. The details of the derivation are essentially identical with those of the equations for the blowing manifolds.

The mathematical equations for the sucking manifolds differ from the corresponding relations for the blowing manifolds for two reasons: first, fluid flows *into* the main tube from the ports; second, the distance along the manifold is measured again from the open end so that the direction of increasing x will be opposite to that of the fluid flow.

If distances are measured from the open end of the manifold, one easily finds that

$$\overset{*}{P}{}'_i - \overset{*}{P}{}^{\circ}_i = - F_0 U_1^{7/4} \Delta y \tag{1.18}$$

$$\overset{*}{P}{}^{\circ}_{i+1} - \overset{*}{P}{}'_i = - \tfrac{1}{2}(U_i^2 - U_{i+1}^2) \tag{1.19}$$

$$U_{i+1} - U_i = - \Delta y \sqrt{\overset{*}{P}{}'_i + \overset{*}{P}{}^{\circ}_{i+1}} \tag{1.20}$$

where

$$\overset{*}{P}{}^{\circ}_i = \frac{g_c}{2k\rho u_0{}^2}(p_0 - p_i^{\circ}) \tag{1.21}$$

Otherwise, the nomenclature is the same as before. Also, if equations (1.19) and (1.20) are combined, one obtains

$$U_{i+1} = \frac{1}{1 - \dfrac{(\Delta y)^2}{2}} \times \left\{ U_i - \sqrt{\frac{(\Delta y)^4}{4} U_0^2 + 2(\Delta y)^2 \left[1 - \frac{(\Delta y)^2}{2}\right] \overset{*}{P}{}'_i} \right\} \tag{1.21}$$

Equations (1.18), (1.19) and (1.21), together with the conditions that at the open end of the manifold,

$$U_0 = 1$$

and

$$\overset{*}{P}{}^{\circ}_i = \frac{M_0{}^2}{2} \tag{1.22}$$

can then be solved by a simple iteration. The solution is again expressible in terms of the three dimensionless parameters M_0, F_0 and Δy.

Finally, the basic equation for the continuous sucking manifold can be derived from the above relations by letting $\Delta y \to 0$ formally, as was done earlier in conjunction with the blowing manifold. Thus, it is found that

$$\left(\frac{d^2U}{dy_2}\right)\left(\frac{dU}{dy}\right) - U\left(\frac{dU}{dy}\right) + F_0 U^{7/4} = 0 \tag{1.23}$$

with the conditions that at $y = 0$

$$U = 1 \tag{1.24}$$

and

$$\frac{dU}{dy} = - M_0$$

The basic equations for the manifolds, when solved numerically with a digital computer or otherwise, enable one to predict the rate of discharge through the ports as a function of the distance along the main tube. Any proper design of the manifold demands that this rate of discharge be as uniform as possible. This, as will be shown by the numerical calculations, can be realized when M_0, which is related to the pressure at the open end of the manifold, is made large.

Calculated Manifold Flow Distributions

Owing to the fact that the one-dimensional flow pattern for continuous manifolds depend on only two parameters, M_0 and F_0, whereas a third parameter, Δy, is needed for manifolds with finite numbers of ports, calculated flow distributions for the former type will be presented more completely than those for the latter. Figure 6 shows a typical set of curves resulting from computer calculations for a family of blowing manifolds characterized by $M_0 = 1{\cdot}0$ and by various values of F_0. From its definition, M_0 can be seen to represent the ratio of fluid pressure to specific kinetic energy (or momentum flow) at the entrance. The pressure rise is therefore expected to be smaller the greater M_0 is. On the other hand, F_0 is proportional to the wall friction factor; the greater its magnitude the greater will be the tendency for pressure to fall in the direction of flow. For each value of M_0 there should be a value of F_0 that will cause the momentum and friction effects to be about equal on the average. The calculations show, however, that no pair of values of M_0 and F_0 gives a perfectly uniform

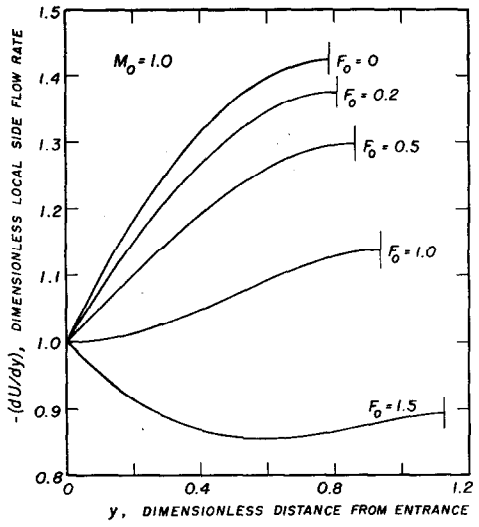

FIG. 6. Calculated side-flow distributions for a group of continuous "blowing manifolds" with closed ends.

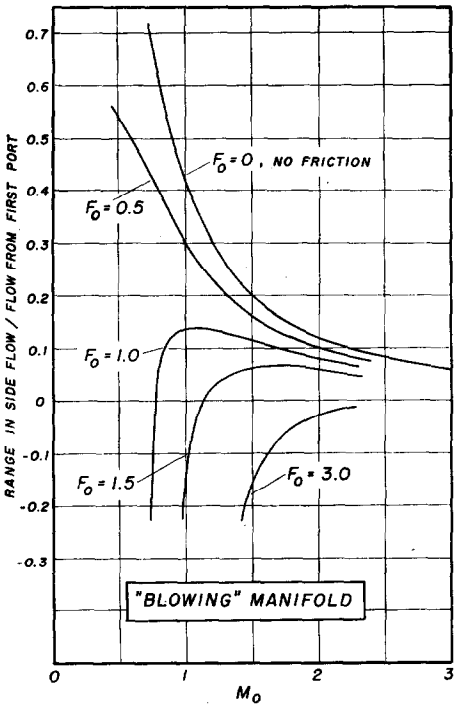

FIG. 7. Results of calculations for continuous "blowing" manifolds showing difference of extreme values of side flow. When ordinate is negative maximum flow occurs at entrance; when ordinate is positive maximum flow is at closed end and minimum may be at entrance or at an intermediate position.

sideways flow. If the side flow is the same at the entrance and the closed end, as will the case for $M_0 = 1{\cdot}0$ and $F_0 \sim 1{\cdot}3$, for example, according to Fig. 6, the side-ways flow rate will have a minimum value near the middle of the manifold.

Fig. 7 shows the condensed results of calculations similar to those just described by plotting the difference in the extreme values of the side flow rate against M_0, with F_0 as a parameter. The figure shows that, although the flow distribution may be approximately uniform at any value of M_0 provided the value of F_0 is properly chosen, the distribution is best in all cases when the value of M_0 is large. M_0 can be varied by a designer most readily by varying the entrance velocity through a change in the cross-section. Large cross-sections lead to low velocities and, thus, to large values of M_0. F_0 contains factors that are not subject to independent variation in a design, except for α, the ratio of port area per manifold unit to the inside surface area. Often this can be made as small as desired by spacing

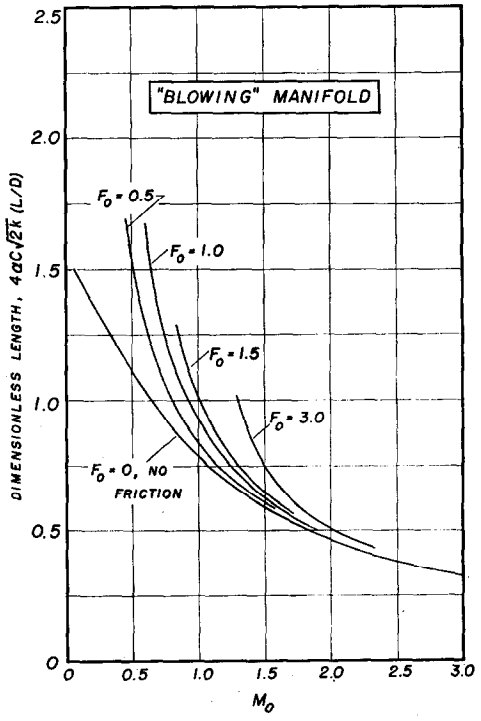

FIG. 8. Results of calculations for continuous "blowing" manifolds showing dimensionless length required to discharge total input stream.

the side outlets far apart. Presumably, also, extra friction devices could be installed between the ports, if necessary.

Fig. 8 shows another result of the same set of calculations that led to Fig. 7. The dimensionless length of the manifold is plotted against the same two parameters. The length required to discharge all the input stream from a manifold with a closed end is seen to depend strongly on M_0. The effect of F_0 is strong if M_0 is small, the required length being greater when friction is present because generally the flow is most non-uniform when friction is absent and the greater side flow rates near the closed end cause the fluid to be discharged more quickly. If the side flow were perfectly uniform, a simple material balance shows that

$$4\alpha C\,(2k)^{1/2}\,(L/D) = M_0^{-1} \equiv \left(\frac{k\rho u_0^2}{g_c\,\Delta p_0}\right)^{1/2} \qquad (1.25)$$

Most of the dimensionless lengths read from Fig. 7 are larger than this, owing to the imperfect distribution. Equation (1.25) shows that when the flow is nearly uniform k has little effect on L, since it appears on both sides of the equation. On the other hand, since it influences the pressure rise, k has a large effect on the flow distribution.

The dimensionless length shown on Fig. 7 is a direct indication of one of the main features of a manifold. If $C\,(2k)^{1/2} \sim 1{\cdot}0$,

$$4\alpha C(2k)^{1/2}(L/D \sim \frac{\text{total port area}}{\text{cross-sectional area of main tube}}$$

KELLER [5] concluded that this ratio should not exceed unity and that the ratio of length to

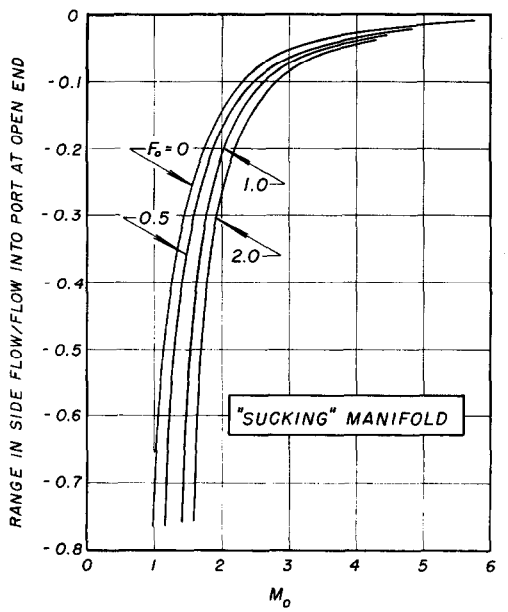

Fig. 9. Results of calculations for continuous " sucking " manifolds showing difference in extreme values of side flow. Maximum flow into manifold always occurs at port nearest open end.

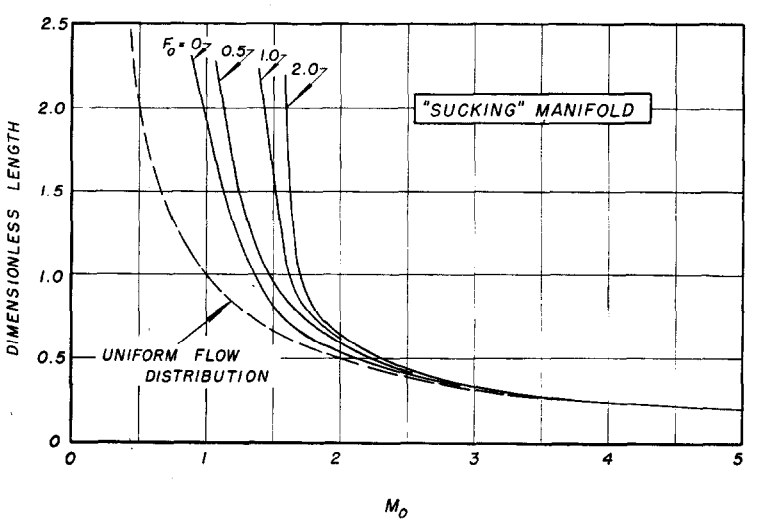

Fig. 10. Results of calculations for continuous " sucking " manifolds showing dimensionless length required to receive total output stream.

diameter should not be greater than 70 for substantially uniform distribution to be obtained. Using $4\alpha C\,(2k)^{1/2}\,(L/D) = 1{\cdot}0$ and $L/D = 70$, $\alpha C = 1/280$. Assuming $f_0 = 0{\cdot}006$, $F_0 = 0{\cdot}84$. This represents one point on Fig. 8 for which $M_0 = 0{\cdot}90$. From Fig. 7 the range in side flow under these extreme conditions permitted by KELLER'S rule is found to be 18 per cent of the flow from the first port. When *smaller* length: diameter ratios are used, however, F_0 and M_0 are reduced and the flow variation is *increased.* The specification of a single pair of maximum allowable values of area ratio and of L/D thus appears to be insufficient to insure good flow control; however, values of M_0 larger than 0·90 usually are needed and ordinarily these will correspond to area ratios less than unity.

Figs. 9 and 10 are similar to the two just discussed, but they apply to sucking manifolds into which fluid flows from an outside, constant-pressure source. Here the friction effect and the momentum effect act in the same direction, causing the pressure inside the manifold to grow smaller in the direction of flow, i.e., toward the open end of the manifold where the fluid leaves. There are no minima in the side flow distribution curves and at a given pair of values of M_0 and F_0 the flow distribution is less uniform than it is for the blowing case. To handle the same quantity of fluid, therefore, a sucking manifold will have a larger cross-section than a blowing manifold if both are to produce similar flow distributions. Moreover the influence of fluid pressure on density has been neglected in the calculations described in this paper and it appears likely that when this additional influence of fluid expansion is allowed for the required area for such manifolds will be even greater than that indicated by Figs. 9 and 10.

EFFECT OF FINITE NUMBER OF SIDE PORTS

The basic equations were derived above in terms of three parameters, M_0, F_0 and Δy. It was only by going to the limit $\Delta y \to 0$ that the differential equations (1.16) or (1.23) were obtained. The results obtained by integrating these equations have been regarded as useful idealizations of flow distributions for actual distributors, although they apply in fact only to flow from a continuous slot of constant width. In this section we return to the non-linear difference equations (1.8), (1.10) and (1.11) for the blowing manifold with a finite number of side ports. By solving the system for various values of Δy but constant values of M_0 and F_0 we determine how many side connections are needed to make the distribution essentially like that for a slot opening.

Fig. 11 shows the results of such calculations, plotted with the same co-ordinates as Fig. 6. The upper curve on Fig. 11 is the same curve as that

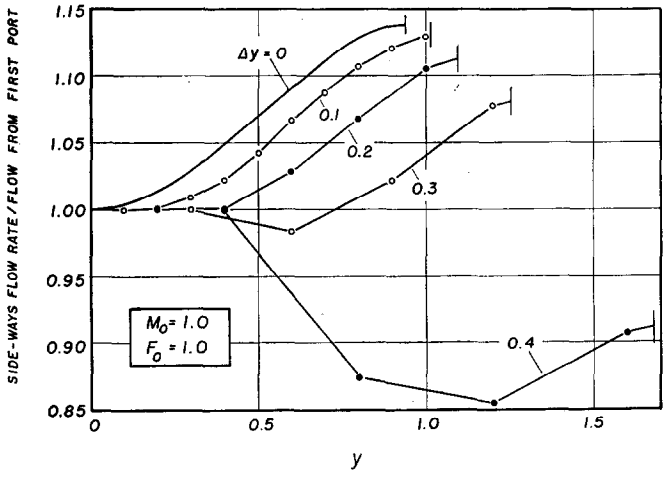

FIG. 11. Effects of finite distance between ports on flow distribution.

shown on Fig. 6 for $M_0 = 1$ and $F_0 = 1$; it evidently applies to the case $\Delta y = 0$. The other curves show the distributions calculated from the difference equations for $\Delta y = 0{\cdot}1$, $0{\cdot}2$, $0{\cdot}3$, and $0{\cdot}4$, corresponding to approximately 10·1, 5·5, 4·2 and 4·1 side ports, respectively. (Since the computation started at the open end of the manifold, where the main fluid stream entered, it did not lead to a precisely zero value of U_i following one port, so that the numbers of ports did not turn out to be integers. This does not destroy the value of the comparison with the solution of the differential equation, however.) Fig. 11 shows that reducing the number of side ports makes the distribution more uniform initially, until the distance between adjacent ports becomes so great that the friction in these sections produces a deep minimum in the sideways flow in the middle of the manifold. Ten side ports produce a distribution that is very nearly like that calculated for a continuous slot.

Fig. 11 also shows that the length of tubing required for the manifold increases as the distance between side ports increases, the ratio of port cross-section to total inside surface of the manifold tube being held constant all the while. Evidently the increasing influence of friction in the manifold tube causes such a reduction in pressure that the distant ports are " starved " for fluid.

Sample Calculation

Suppose that 50 gal/min of water are to be split into ten nearly equal parts by means of a manifold composed of a straight pipe D′ in. in internal diameter to which ten, one-inch, schedule-40 pipes are to be welded at right angles. The manifold will be 10 ft long, the interval between adjacent 1 in. pipes being 1 ft. Calculate the percentage variation in the flow rate through the ten small pipes and the pressure inside the manifold at the entrance for D' equal to 3, 4 and 5 in.

From the stated dimensions and using 1·049 in. for the inside diameter of the branch lines,

$$\alpha = \frac{10 \times 1{\cdot}049^2 \times \pi}{4 \times \pi \times D' \times 10 \times 12} = 0{\cdot}0229/D'$$

$$4\alpha C\,(2k)^{1/2}\,(L/D) = 4(0{\cdot}0229/D')\,(0{\cdot}6)\,(2 \times 0{\cdot}6)^{1/2}\,(10 \times 12/D') = 7{\cdot}22/(D')^2$$

$$u_0 = \frac{50 \times 231 \times 4 \times 144}{1728 \times 60 \times \pi\,(D')^2} = 20{\cdot}4/(D'^2),\ \text{ft/sec.}$$

$$N_{Re} = \frac{(D')\,(20{\cdot}4)\,(62{\cdot}3)}{(12)\,(D')^2\,(0{\cdot}000673)} = 157{,}200/D'$$

$$F_0 = \frac{(f_0)\,(D')}{(2)^{5/2}\,(k)^{3/2}\,(C)\,(0{\cdot}0229)} = 27{\cdot}7\,f_0\,D',$$

based on $k = C = 0{\cdot}6$. Similarly,

$$M_0^2 = \frac{(32{\cdot}17)\,(\Delta p')\,(144)\,(D')^4}{(0{\cdot}6)\,(20{\cdot}4)^2\,(6{\cdot}23)} = 0{\cdot}298\,(\Delta p')\,(D')^4$$

where $\Delta p'$ is in lb/in² gauge.

Using $D' = 4$ in. to illustrate the calculations, $N_{Re} = 39{\cdot}200$ and $f_0 = 0{\cdot}0063$ for commercial pipes. Furthermore, $F_0 = 0{\cdot}70$ and $4\alpha C\,(2k)^{1/2}\,(L/D) = 0{\cdot}452$. From Fig. 8 the required value of M_0 is 1·86 and from Fig. 7 the fractional variation in the distributed flow is 0·115. Trial of the other two diameters leads to the numerical results shown in the following table:

Manifold diameter, D′ (in.)	F_0	$4\alpha C\,(2k)^{1/2}\,(L/D)$	M_0	*Per cent range in side flow*	$\Delta p'$, (lb/in²)
3	0·50	0·80	1·05	28	0·046
4	0·70	0·45	1·86	11	0·045
5	0·91	0·29	2·52	5	0·034

Observed Flow Distributions

In order to compare the predicted flow non-uniformity with experimentally observed distributions several tests were carried out using equipment, described in a previous section, that had been employed in the determination of the pressure-rise coefficient, k. For this purpose many of the side tubes were allowed to discharge simultaneously and the rate of flow through each tube was measured by means of a sensitive micromanometer and a Pitot tube made from hypodermic tubing. Pressures at intermediate points on the bottom of the main channel were also observed using the micromanometer.

Typical data for one run are shown by Fig. 12, which represents a run in which all twenty-four of the ports were opened and the valve downstream from the last port was completely closed. As shown by the figure, the fluid pressure decreased in the direction of flow owing to fluid friction as the air approached the first port. Then, within the area in which ports were discharging the pressure fell to a shallow minimum and rose owing to the fluid momentum effect described above. Finally, after the last port the pressure was constant because flow had ceased in the manifold, the last hole having discharged the last portion of the main stream.

The upper plot on Fig. 12 shows the corresponding increase in flow from the manifold. The

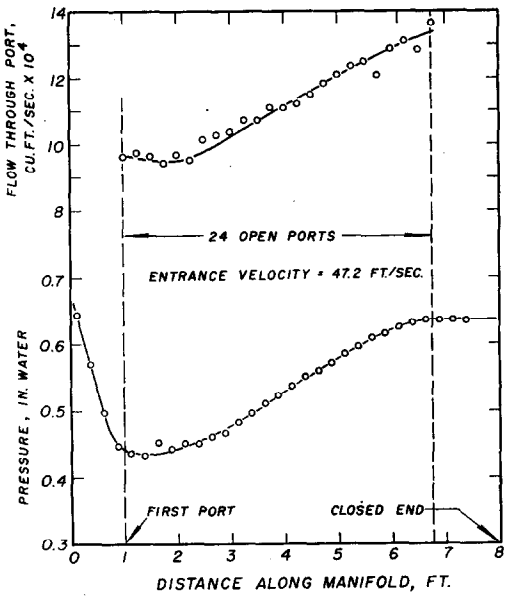

Fig. 12. Typical data from test of "blowing" manifold curves show increase in side flow owing to increased internal manifold pressure near closed end.

fractional variation in sideways flow is seen to be (13·2-9·6)/9·6, or 0·38. This is one of the figures appearing in Table 1, which compares the observed departure from flow uniformity with the value predicted from Fig. 7 at the values of M_0 and F_0 corresponding to the existing entrance

Table 1. *Summary of flow distribution data from experimental manifolds.*

No. holes open	M_0	F_0	*Max. range of side flow, % of of flow from first port*		*Dimensionless length of manifold* $4\alpha C(2k)^{1/2}(x/D)$	
			Observed	*Predicted*	*Observed*	*Predicted*
8	2·79	2·60	6 ± 1	3 ± 2	0·29	0·28
16	1·38	1·30	12 ± 1	9 ± 1	0·77	0·69
16	1·20	0·65	15 ± 2*	8 ± 1	0·97*	0·74
32	0·77	0·65	33 ± 1	30 ± 5	1·55	1·08
12	1·32	1·03	14*	12	0·95*	0·91
24	0·83	0·50	38	39	0·82	0·92
24	0·80	0·50	30*	40	1·55*	1·00

*Manifold open at downstream end in these runs. Figure tabulated is found by approximate extrapolation of observed flow distribution to point beyond end of manifold where inside stream would have been exhausted.

velocity and excess pressure and to the values of k and C found in the previous single-port experiments.

Table 1 also includes three comparisons of observed and predicted quantities in which the manifolds tested were not completely closed on the end. Since Figs. 7 and 8 apply only to closed-end manifolds it was necessary to extrapolate the observed port flow rates in these cases to hypothetical positions beyond the end of the actual manifold to the point where the flow rate of the main stream would have been expected from a similar extrapolation to have reached zero. Possibly because these extrapolations had to be made in a somewhat arbitrary manner the comparisons in the table are not quite as good as those for the four "normal" runs. In most cases the predicted and observed dimensionless lengths also agreed satisfactorily, though one of the "normal" runs seems to show a large deviation for no apparent reason.

Generally speaking the table shows that expected and observed flow distributions agreed approximately, justifying the expectation that Figs. 7 and 8, and presumably also Figs. 9 and 10 can be used for the design of piping systems.

Acknowledgement—The authors wish to express their appreciation to Messrs. D. EWING and T. FESTIN, respectively undergraduate and graduate students at the University of Delaware, who assisted with the experimental work. Computing facilities were made available by the University of California, Berkeley, California, and by the Computing Centre at the University of Delaware.

NOTATION

The following nomenclature is employed:

p°_i = the pressure at the left end of the straight tube-section i

p_i' = the pressure at the right end of the straight tube-section i

p_0 = the uniform pressure outside the discharge ports

u_i = the velocity in the straight-tube section i

D = the diameter of the main tube

$\Delta x = x_{i+1} - x_i$ = the distance between adjacent discharge ports

α = fraction of internal area of the tube that is occupied by discharge ports, assumed uniformly spaced along the tube

$\alpha\pi D\Delta x$ = the discharge area of a port

f = the Fanning friction factor

ρ = the fluid density

C = the discharge coefficient for the orifice equation, applied to the side outlets

L = the distance between the closed end and the entrance to the manifold

REFERENCES

[1] BABCOCK B. D. *B.S. Thesis* University of Delaware, 1952.

[2] BERMAN A. S. *J. Appl. Phys.* 1953 **24** 1232.

[3] CADIGONE C. *Appl Sci. Res.* 1953 **A4** 76 *Hague.*

[4] DOW W. M. *Mech. Engng.* 1950 **72** 748.

[5] KELLER J. D. *Trans. Amer. Soc. Mech. Engrs.* 1949 **71** 77.

[6] ROUSE H. *Engineering Hydraulics*, p. 437. J. Wiley and Sons, New York 1950.

[7] SOUCEK E. and ZELNICK E. W. *Trans. Amer. Soc. Civil Engrs.* 1945 **110** 1357.

[8] WEISSBERG H. L. Report No. K-1187, Mar. 29, 1955, Carbide and Carbon Chemicals Co., Union Carbide and Carbon Corporation, K-25 Plant, Oak Ridge, Tenn.

[9] ZIJNEN B. G. and VAN DER HEGGE, *Appl. Sci. Res. Hague* 1952 **A3** 1944.